Review

Overview and Progress of GNSS Anti-multipath Antenna Designs

Jianming Dong[1]*, Qiang Hua[2]

[1] Beijing Institute of Technology; olivierdjm@163.com
[2] University of Huddersfield; Q.Hua@hud.ac.uk
Corresponding Author: olivierdjm@163.com,

Received date:29/08/2023; Accepted date:28/09/2023; Published date: 30/09/2023

Abstract: This article provides a comprehensive review of recent applications of GNSS anti-multipath antenna. Emphasis is placed on the role of anti-multipath antenna in GNSS. A brief summary of the current anti-multipath antenna in satellite-based navigation systems is provided and also the GNSS anti-multipath antenna plays a key role is emphasised, which will help in getting a better understanding of the requirements on the various performance parameters of a GNSS antenna. In addition, we review GNSS anti-multipath antenna design strategies and specific design examples that highlight the application of various types of GNSS anti-multipath antenna. Ultimately, this articles seeks to demonstrate the value of GNSS anti-multipath antenna design insights for antenna engineering and look toward promising new research directions for GNSS antenna research.

Keywords: anti-multipath; GNSS; choke ring; pinwheel antenna; multifunctional antenna

1. Introduction

The antenna is the first component of a Global Navigation Satellite System (GNSS) receiver that processes signals received from multiple GNSS satellites. Because it operates both as a spatial and a frequency filter, it can have a significant influence on many aspects of the satellite navigation system, which requires that it satisfy important performance requirements [1].

1.1. Role of an anti-multipath antenna in GNSS

One of the most important requirements of GNSS antenna is that the antenna provide the minimum gain and the broad beamwidth required by the receiver to acquire a minimum of at least four satellites; additionally, some of these acquired satellites must also be at low elevation angles to achieve the best geometrical dilution of precision (GDOP) [2]—a critical parameter that affects the accuracy of all GNSS measurements [3]. The bandwidth of the antenna must also be sufficient for processing all available GNSS signals—GNSS frequency now ranges from 1.1 to 1.6 GHz, and for many applications wideband antennas will replace the old legacy antennas that only covered the Global Positioning System (GPS) or the Russian GNSS, GLONASS [4]. The antenna must also have minimal backlobes, a sharp cutoff at low altitudes close to the horizon, and a good polarization axial ratio to ensure good rejection of multipath and interference [5]. The antenna designs that are used to mitigate these multipath effects are explored. The phase offsets, phase center variations, and carrier phase windup of the antenna can restrict on the accuracy of differential GPS measurements. Hence, they must

be correctly calibrated and taken into consideration. An antenna for commercial devices, such as smartphones and personal digital assistants (PDAs), should be small and light. It should also be able to provide low weight and cost. These are some of the factors that are considered when choosing an antenna for commercial applications [1].

Since the signals received from the satellites are very weak, the threats of interference and jamming are ever-present in GNSS. Some GNSS applications demand very high gain antennas, which are necessary for testing or for more thorough satellite signal monitoring and troubleshooting. In addition to other types of array antennas, these high gain antennas also include helical antennas and beamforming antenna arrays, which enable multiple beams to be steered at particular satellites to achieve the highest carrier-to-noise ratios while minimizing multipath and interference.

The antenna is often required to satisfy multiple and often conflicting requirements mandated by the specific system for which the antenna is intended. For example, in order to acquire the maximum possible number of visible satellites, most GNSS antennas are required to have a very broadbeam with appropriate gain in the upper hemisphere down to a low elevation masking angle. However, the antenna is also simultaneously required to operate as a spatial filter with a sharp cutoff in gain at elevations immediately below the masking angle to reduce susceptibility to multipath and interference. A sharp cutoff at low elevations may also not be desirable for certain GPS antennas located on certain platforms, such as ships, which can experience significant pitch and roll caused by heavy sea conditions, as well as antennas located on aircraft, particularly during critical takeoff and landing operations when the aircraft is likely to undergo similar changes in its orientation in the pitch, roll, and yaw planes. High-profile antennas such as quadrifilar helices provide good gain at low elevation angles but may be too tall for aircraft that require low profile antennas for reduced drag and for interference reduction [1].

1.2. Multipath Errors in GNSS Measurements

The measurement of pseudorange and carrier phase—the two most important observables obtained from GNSS measurements—are influenced by several errors such as propagation errors experienced by the signal as it travels from the satellite to the receiver antenna. The largest contribution to such errors comes during propagation through the troposphere and the ionosphere [6]. In addition, the GNSS signal can experience multipath, where both the direct signal and one or more reflected signals arrive at the antenna causing errors in phase and amplitude. Since the strongest multipath signals generally arrive in directions close to the horizon or below it, the antenna needs to be designed to reduce backlobes. Antenna using choke ring, EBG or resistivity tapered ground planes help in the reduction of such backlobes [1].

This paper is organized as follows. Section I introduces the role of anti-multipath antenna in GNSS and multipath errors in GNSS measurements. A variety of GNSS anti-multipath antenna design, its operational theory and recent research development are discussed in detail in Section Ⅱ. Section Ⅲ concludes this paper.

2. GNSS Anti-multipath Antenna

2.1. Methods of Multipath Mitigation

Spatial processing and time-domain processing are the two basic categories of processing against slowly changing multipath. Spatial processing isolates the direct-path received signal by combining antenna design with known or partially known signal propagation geometry parameters. In contrast, time domain processing operates on the multipath-corrupted signal within the receiver to mitigate the multipath on the measurements before they are applied to

the position, velocity and time (PVT) solution technique [2].

Two of the main factors that affect the multipath error are the magnitude and delay of the multipath signal, relative to the direct signal received at the user antenna from the GNSS satellite. Placing the reception antenna directly at ground level is a simple, but frequently unpractical, strategy for minimizing ever-present ground signal reflections [7]. This causes the point of ground reflection to be essentially coincident with the antenna location so that the secondary path has very nearly the same delay as the direct path. Generally speaking, the antenna should be placed at a high enough elevation angles. It should be noted that the higher the antenna is mounted from reflecting surfaces, the greater the multipath delay, which will intern, increase the multipath error, however, at the same time, the multipath reflection will enter the antenna at a more negative elevation angle, which will result in a decrease in multipath error [1].

The effects of edge diffraction have been reduced by designing various types of modified ground planes. These include choke-ring ground plane, EBG ground plane, rolled edge ground plane, and the resistivity tapered ground plane. The Mitigation of ground plane effects on performance of GNSS antennas, which is described in detail, are as follows.

2.2. Choke Ring Antenna

2.2.1 DM Antenna and Choke Ring

The choke ring-based antenna was originally introduced to the GNSS community by the Jet Proposal Laboratory (JPL) and was used with a Dorne & Margolin (DM) dipole-based GPS antenna element [8]. For the purpose of mitigating multipath, the choke ring is essentially a shaped ground plane made of conductive material forming a series of concentric circular troughs. The picture of a typical choke-ring antenna used in GNSS applications is shown in Figure 1.

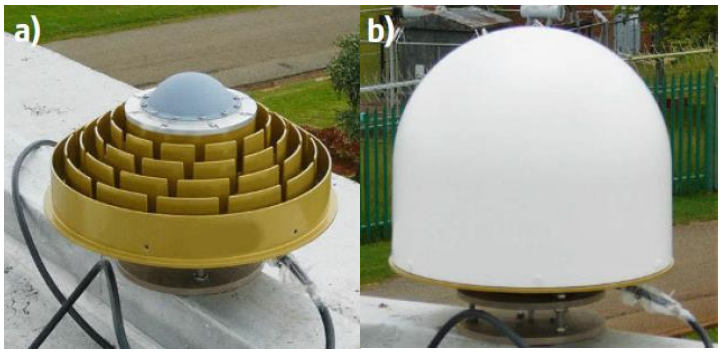

Figure 1. Choke-ring antenna without (a) and with (b) protective radome [3].

The Dorne and Margolin (DM) antenna is widely used for GNSS geodetic applications. It is a compact right-hand circularly polarized (RHCP) antenna based on a half Alford loop with a wideband response [6].

A critical issue is the reduction of multipath interference, which has a direct impact on the performance (accuracy of position determination) of the GNSS antenna front-end; a right hand circular polarized (RHCP) satellite signal reflects at the earth's surface, partially changes from RHCP into left hand circular polarized (LHCP), and can arrive at the backside of the antenna, causing multipath interference. A solution to this problem is reducing the reception of LHCP signals by means of shielding the antenna from those signals. A problem arises however when a metal plate is simply used [Figure 1(a)]; currents flowing on the ground plane strongly influence the radiation properties of the antenna, having a severe impact on its phase center

stability and axial ratio. To prevent this, choke rings are commonly applied. The electromagnetic field of the reflected signal in the vicinity of the choke ring ground plane (S), as shown in Figure 1(b),can be considered as the sum of two field waves (primary wave and secondary wave). The purpose of the choke ring ground plane is to mitigate the primary and secondary reflected signals so that the direct signal remains dominant. If the amplitude of the primary and the secondary waves are equal, and the phase difference between them is 180, then the two components of the reflected signal cancel each other out at the antenna output, therefore suppressing multipath interference [8]. A given choke ring functions optimally within a specific frequency range for which the choke ring shows a resonance behavior. In reality this means that the depth of the grooves must be close to the quarter of the wavelength. There are various technologies available to achieve multifrequency operation of choke rings [9].

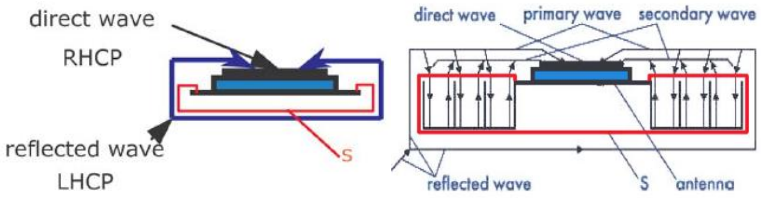

(a) (b)

Figure 2. Multipath interference [8].

Choke rings are a well known method for shaping the radiation pattern to reduce multipath and stabilize the phase center, consisting of three to five narrow concentric metallic circular corrugation, with ring depth slightly greater than a quarter wavelength and a width between rings slightly greater than an eight wavelength. The geometric variation of the ground plane reduces gain to the GNSS SVs at lower elevation angles. Multipath and interference signals below the horizon (i.e. 0° elevation angle) are diffracted by the choke rings. The diffractions will induce secondary currents on the choke ring structure, and some current will find its way to the antenna elements but the amount of current will be substantially reduced if the choke ring structure not been present [10].

The physical dimensions of the choke ring ground plane structure can be optimized for a single GNSS frequency, or designed to be a compromise in performance for multiple GNSS frequencies that are several hundreds of megahertz apart [11].

As the radiating element, various antenna designs can be utilized at the center of the choke ring. Initially, a domed radome housing was commonly used to enclose a dipole-based GPS antenna. Multifrequency patch antennas are also commonly placed at the center of GNSS choke ring antennas.

To help mitigate multipath error, variations in the traditional choke ring structure have been utilized, including a variation of depth [12],use of a single choke ring [13],and use of a 3D choke ring structure [14]. For multipath and interference mitigation, the latest generation of 3D choke ring structures provide for a more uniform gain in the upper hemisphere and better suppression of the gain at negative elevation angles.

2.2.2 Recent Development

In recent years, there have been some reports on the improvement and enhancement of choke ring to anti-multipath.

To solve the problem of narrow bandwidth of dielectric choke rings, a novel low-profile grooved-dielectric choke ring with dual-band surface impedance resonance is proposed and

experimentally demonstrated in [16][17][18]. The proposed structure is designed by engineering the surface impedance of a dielectric-based choke ring to introduce two resonant frequencies around the global navigation satellite system (GNSS) bands of L2 (1227.60 MHz) and L1 (1575.42 MHz). This provides capacitive surface impedances around both bands simultaneously, which is essential for efficient surface wave suppression for higher multipath rejection performance. An in-house choke ring prototype of the proposed design is tested with the widely used Dorne and Margolin antenna to demonstrate the proposed surface impedance engineering principle. A high multipath rejection in both GNSS bands is experimentally confirmed with comparable performances to an otherwise bulky, heavy, and expensive conventional metallic choke ring. When compared to the conventional choke ring, the proposed FR4 design provides 58% reduction in height and 26% reduction in diameter and is an attractive low-cost solution for high-performance GNSS applications [15].

In [15], the dual-resonance can be achieved by using two different dielectric fillings, with FR4 (εr = 4.4) and Neltec NX9240 (εr = 2.4), inside the choke ring at optimal locations, where an additional surface impedance resonance is created at L1, in addition to the resonance at L2, as shown in Figure 3(a). The dimensions of the structure required to achieve the dual resonance at L2 and L1 are as follows: a = 280 mm, s = 10 mm,d = 29.2 mm, and t = 3 mm. Surface impedance resonance can be optimized at both L2 and L1 by varying the dielectric constants and their locations. As illustrated in Figure 3(b), the same dual-band response can be obtained by replacing Neltec NX9240 with FR4 with air grooves. The dimensions of the structure required to achieve the dual resonance at L2 and L1 has the following dimensions: a = 280 mm, s = 10 mm, d = 29.2 mm, dg = 15 mm, w = 4 mm, and t = 3 mm. Introducing the grooves reduces the effective εr in the cavities. Width, w, and depth, dg, of the groove were determined empirically to obtain the desired response [15].

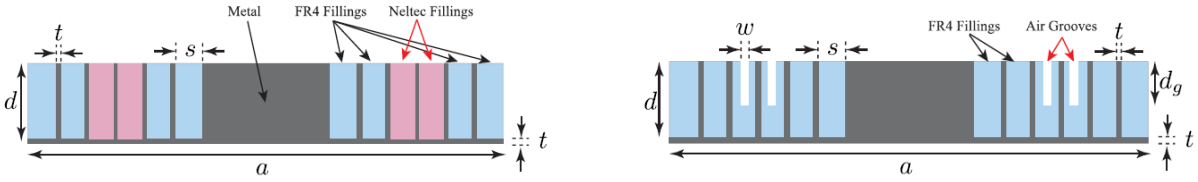

(a) (b)

Figure 3. Two electromagnetically equivalent dielectric choke rings. (a) Multidielectric choke ring made by filling corrugation cavities with FR4 and Neltec NX9240. (b) Proposed grooved-dielectric choke ring made by filling corrugation cavities with FR4 with grooves [15].

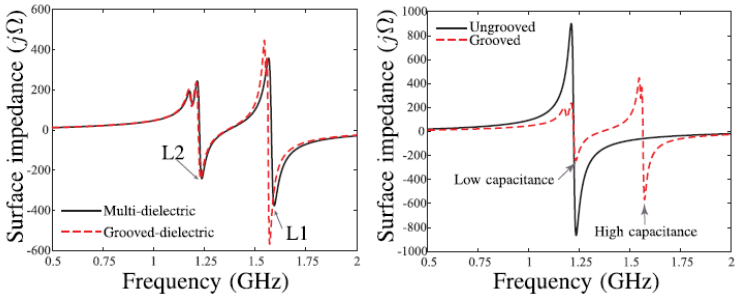

Figure 4. (a) Surface impedance of the multidielectric design and the proposed grooved-dielectric design. (b) Surface impedance comparison between ungrooved and proposed grooved FR4 choke rings [15].

Figure 4(a) demonstrates that the surface impedance of the grooved-dielectric design is virtually comparable to that of the multidielectric design. Figure 4(b) depicts a comparison of the surface impedances of the ungrooved FR4 choke ring and the grooved FR4 choke ring.

While introducing the grooves adds a second resonance around L1 with a high capacitive response, it also results in a lower capacitance at L2 compared to the original design [15]. In this sense, the proposed structure has a tradeoff where it improves the performance at L1 at the expense of degradation at L2. While this appears to be a disadvantage of the proposed choke ring, it will be demonstrated that the surface impedances obtained in both bands are capacitive enough to offer good surface wave suppression in both bands. Top view of the fabricated grooved-dielectric choke ring with the DM antenna, as shown in Figure 5(a). Measured return loss is shown in Figure 5(b).

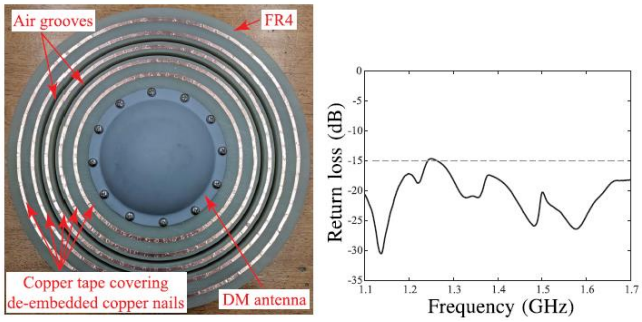

(a) (b)

Figure 5. (a) Top view of the fabricated grooved-dielectric choke ring with the DM antenna. (b) Measured return loss [15].

In [16], a novel technique for miniaturizing of corrugated structures is presented, and multifolded corrugations (MFCs) are introduced. The miniaturization is achieved by implementing multiple folds or slits inside corrugations. The proposed miniaturization technique is utilized to model using the modal expansion method. The surface impedance of the proposed MFCs is precisely modeled by an analogous circuit that is extracted. A time-efficient design procedure is presented based on the equivalent circuit model, and a dual-band double-folded substrate integrated choke ring (DFSICR) structure is designed to suppress the propagation of surface waves over the main global navigation satellite system (GNSS) frequency bands: L1 (1573–1587 MHz) and L2 (1215–1240 MHz). The DFSICR has considerable multipath mitigation capabilities that are comparable to those of a traditional choke ring while doing away with its disadvantages, such as its bulk, weight, expensive construction, and inability to interface with printed circuit board (PCB) structures. In comparison to the conventional choke ring, a sample design displays miniaturizing of 85% in height and 38% in diameter. With respect to the traditional choke ring, a prototype made from FR4 laminates shows a weight reduction of more than 90% [16].

(a) (b)

Figure 6. (a) Double-folded SICR design. (b) Equivalent circuit of the double-folded SICR [16].

Double-folded SICR design and its equivalent circuit are shown as Figure 6. Expanded view and cross section view dual-band DFSICR are shown as Figure 7. Top view of top laminate, middle laminate, bottom laminate, and assembled structure are shown as Figure 8.

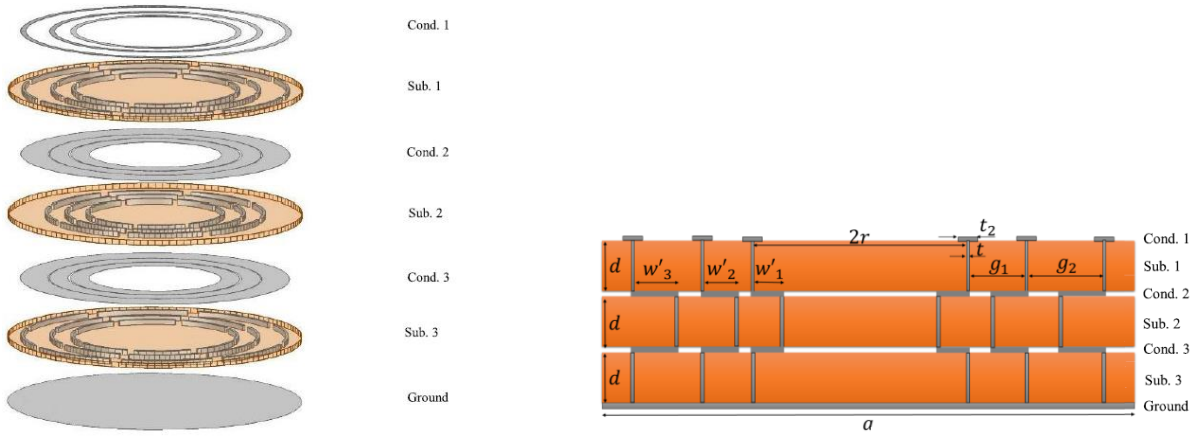

(a) (b)

Figure 7. Dual-band DFSICR. (a) Expanded view. (b) Cross section view [16].

(a) (b) (c) (d)

Figure 8. Top view of (a) top laminate, (b) middle laminate, (c) bottom laminate, and (d) assembled structure [16].

Table 1 compares the proposed configuration to various multipath mitigating ground structures in order to highlight the benefits of the proposed DFSICR. In this comparison, three EBG structures designed for GNSS applications are compared with the proposed DFSICR in addition to the conventional choke ring [18] and the dual-band dielectric-loaded choke ring reported in [16].

Table 1. Comparison between the proposed DFSICR and other multipath mitigation ground structure [16].

Reference	Frequency	Technology	Material	Size	Height	3dB ARBW	FBR(dB)
[15]	L1	EBG	Foam(ε_r=1)	300(1.56λ)	300(1.56λ)	140	22
[17]	L1	EBG	Not Named (ε_r=7)	300(1.56λ)	300(1.56λ)	170	20
[16]	L1,L2	EBG	Foam(ε_r=1)	300(1.56λ)	300(1.56λ)	40-60	24-27
[16]	1.15-1.65GHz	Choke Ring	Hollow corrugation(ε_r=1)	300(1.56λ)	300(1.56λ)	160-180	23-27
[17]	L1,L2	Choke Ring	FR4(ε_r=4.4)	300(1.56λ)	300(1.56λ)	90-160	17-22
This work	L1,L2	DFSICR	FR4(ε_r=4.7)	300(1.56λ)	300(1.56λ)	160-180	20-25

As can be seen, the EBG structures presented in [19] and [20] provide good front-to-back ratios and promising 3 dB ARBW with a relatively low height; nevertheless, they only cover one of the GNSS frequency bands. Additionally, they have lateral dimensions that are about 30% larger than the DFSICR. The EBG structure introduced in [11], which is a modified version of [20], shows a dual-band behavior and a good front-to-back ratio; however, it suffers from

very large area consumption due to the larger size of its dual-band unit cell. Furthermore, it exhibits a very narrow 3 dB ARBW. On the other hand, in comparison to the aforementioned EBG structures, the dielectric-loaded choke ring presented in [21] demonstrates a generally better performance with smaller lateral dimensions. Despite this, the height of the dielectric-loaded choke ring remains still significantly high, and the performance over the lower frequency band requires improvement. The DFSICR developed in this work, however, outperforms the dielectric-loaded choke ring and performs fairly similarly to the conventional choke ring, while providing significant size and weight reduction. The DFSICRs are 85% and 67% smaller in height than the traditional choke ring and dielectric-loaded choke ring, respectively. Additionally, the DFSICR displays size reductions in diameter of 38% and 20% in comparison to the aforementioned designs. Moreover, it demonstrates a weight reduction of more than 90% when compared to the conventional choke rings. The weight of the DFSICR is less than 0.5 kg, whereas the weight of a traditional choke ring structure weighs roughly 5 kg. As a result, the proposed DFSICR demonstrates a tremendous potential to be employed in GNSS systems that mitigate multipath [18].

2.3 Noncutoff Corrugated Ground Plane Anti-multipath Antenna

The non-cutoff choke ring employs a different approach than the traditional choke ring, in which surface waves are induced to destructively interfere (i.e. in the non-cutoff zone) rather than being suppressed, as is the case with conventional choke rings [5]. This reduces the depth of the corrugations and the diameter of the choke ring.

A corrugated ground plane with corrugation depth less than λ=4 is presented in [19] to accomplish multipath mitigation at low-elevation angles. The ground plane, as shown in Figure 9, achieves the surface wave suppression in a different manner than traditional choke-ring. Rather than forming a high-impedance zone surrounding the antenna, the shallow corrugations allow surface waves to propagate toward the ground plane boundary, where they become out of phase with the line-of-sight signals and are canceled [6].

Although the simulation and measurement results presented in [18] show that the shallow corrugations can achieve respectable multipath mitigation performance, the ground plane necessitates a higher number of successive corrugations. This results in an increased diameter which partly compensates the benefit of the decreased choke-ring height [6].

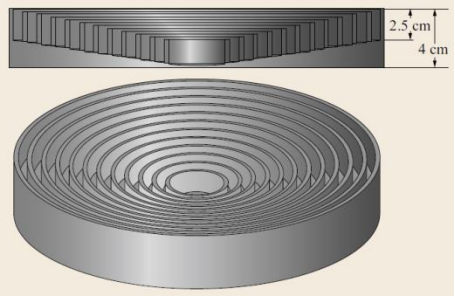

Figure 9. Noncutoff corrugated ground plane for GPS antennas.

2.4 Cross Plate Reflector Ground Plane Anti-multipath Antenna

The design of the innovative cross-plate reflector ground plane can be easily explained by using fundamental electromagnetic theory [6]. Figure 10(a) depicts two types of oblique plane TEM waves; TE (TE to z) and TM (TM to z) with positive x-direction propagation vectors. It is well known from electromagnetic theory that a flat perfect electric conductor (PEC) sheet will cancel out any type of plane waves on its surface if the E-field vector of the propagating wave is parallel to the PEC surface. As a result, because the E-field vector is perpendicular to xy

plane, a flat metal sheet in x–y-direction will hinder the propagation of TE waves but cannot cancel TM waves. A ground plane geometry, on the other hand, where the PEC sheets are arranged in such a way that the E-field vectors of both types of plane waves are parallel to the PEC surface can effectively impede their propagation [6].

A prototype implementation of a dual-band CPRGP antenna employing a shorted annular ring antenna element is presented in [22]. The photo of antenna prototype integrated with cross-reflector ground plane is shown as in Figure 10 (c). The preceding concept is further clarified in Figure 10(b), which depicts a section of the CPRGP structure [23]. The conditions for the waves are provided by the thickness of the top surface and the flat metal bedding, whereas the similar conditions for the TM waves are provided by the vertical plates. Therefore, it can be concluded that if the propagation vector is parallel to the ground plane surface, the CPRGP can accommodate both forms of TEM waves (TE and TM) and can cancel out both of them.

It is discussed in [24] how to create a cross plate reflector ground plane (CPRGP) for multipath mitigation. Here, the antenna element is surrounded by a square with crossed sidewalls, as shown in Figure 10 (b). Other than a flat perfect electric conductor, which only cancels the transversal electric (TEz) waves, the cross plate reflector also cancels the transversal magnetic (TMz) waves. By doing so, it is possible to reduce the overall ground plane thickness to less than λ/4, that is, approximately half that of a conventional choke ring.

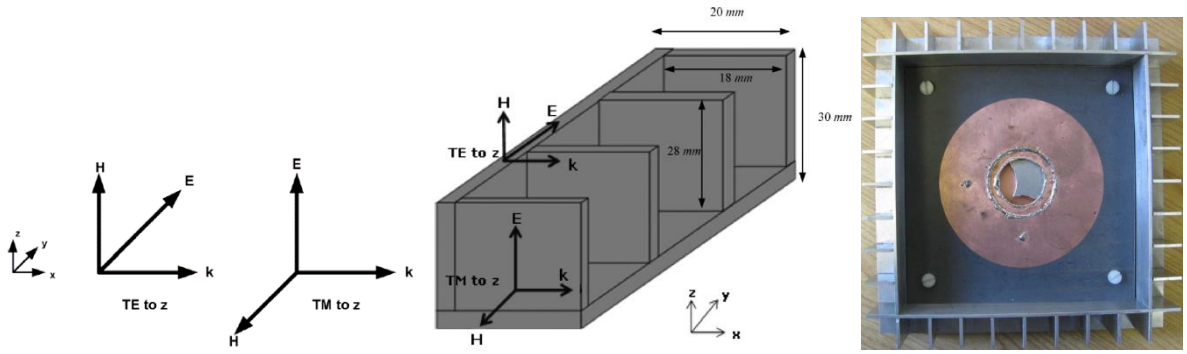

(a) (b) (c)

Figure 10. (b).Vector representation of TE_z and TM_z waves on the cross-reflector ground plane surface. (c). Antenna prototype integrated with cross-reflector ground plane [22].

2.5 Rolled Edge Ground Plane

The rolled edge ground plane is shown in Figure 11.In this design, the signals diffracted from the sharp edges of the ground plane are prevented from affecting the performance of the GPS antenna by rolling the edge underneath the ground plane [25]. Despite being a larger ground plane than either the choke-ring or the EBG, this one is less expensive and easier to build [26],[27].

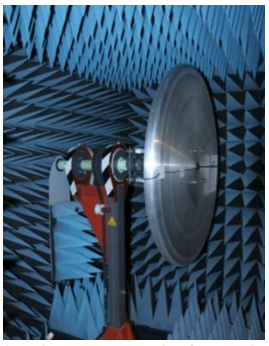

Figure 11. Rolled edge ground plane for GPS antennas.

At the higher elevation angles, the rolled edge ground produces lower LHCP cross polarization levels. Unfortunately, the rolled edge ground plane does not provide significant suppression of sidelobe levels in the lower hemisphere [6]. Because of creeping wave diffraction around the rolled edges of this type of ground plane, this occurs. These backlobes can be suppressed by applying radar absorbing material (RAM) to the rolled edge surface, but this will increase both weight and cost [22]. This form of ground plane would only be useful for precisely measuring the gain of a GPS antenna in an anechoic environment where multipath effects are not a major problem [6].

2.6 Resistivity Tapered Ground Plane

The usage of resistivity tapered ground planes, whose surface resistance gradually increases from the center to the outer edge of the ground plane, can lessen the impacts of ground plane edge diffraction [28]. For multipath reduction, the GNSS antenna is positioned in the center of a resistivity ground plane. This antenna has significant advantages over other multipath mitigation antennas such as the choke ring ground plane antenna. The resistivity tapered ground plane is made from a thin kapton film with a tapered resistive film of Indium Tin Oxide (ITO) sputtered on it. The surface resistivity of the film varies increases from 0 (perfect conductor) at the center to around 2000 ohms per square at the outer edge in an exponential manner. This resistive film is bonded to a thin plastic plate and hence, can be made very light in weight because of the absence of any metallic parts. Since it does not need quarter wavelength deep choke rings it also has a very low profile. The absence of any machined or stamped metal parts makes this type of ground plane very cost effective and lightweight for many commercial GPS applications. The resistive film can be protected from scratching or other types of mechanical damage by sandwiching it between two plastic protective films. A variety of different tapered resistive material that are currently commercially available can be used for making this type of resistivity tapered ground plane; these other material that can be used such as resistive textiles, resistive composite materials used for RCS reduction in aircraft, and specially developed resistive paints. Since the antenna is comprised of microstrip elements it has a low profile and can be made conformal to the surface of an aircraft .The advantage of this ground plane design is that it can be used over a very broad range of GNSS frequencies ranging from 1.15GHz to 1.6GHz since it does not require concentric circular grooves that are tailored to certain frequency bands as in a choke-ring ground or frequency selective surfaces that can only operate in specific frequency regimes as in the EBG ground plane. The resistivity tapered ground plane is able to suppress both the diffraction ripples in the antenna pattern seen at higher elevation angles in the conventional metal ground plane measurements as well as reduce the antenna backlobes of this antenna to below -27dBic.This is a reduction in sidelobe level of about -12dB when compared to that obtained with a conventional metal ground plane.

The Trimble Zephyr GNSS antenna is a planar-type GNSS antenna that implements advanced technologies to help mitigate multipath for mainly geodetic and reference ground station applications [29][30]. The Zephyr antenna utilizes a six-feed patch antenna design with a resistively tapered ground plane, where the surface resistance increases as the distance from the center of antenna increases to provide for enhanced performance and multipath mitigation [31].The method used for the Trimble Stealth Ground Plane is one whereby the e-field of the electromagnetic wave is cut off before it can reach the GPS antenna element [32].This is achieved through the use of a material in which the sheet resistivity increases exponentially along any radial line out from the antenna element to the edge of the ground plane [33]. The utilization of this material offers the advantages of being lighter in weight and less expensive than conventional ground plane designs [34]. As the name suggests, the material was developed out of research conducted as part of the development of the Stealth

aircraft [35][36].

2.7 Convex Impedance Ground Plane Anti-multipath Antenna

An impedance surface parallel to the antenna ground plane is produced by the integration of the choke-ring ground plane with an antenna creates [8]. Although this enhances the antenna's capability for multipath mitigation, it also reduces the antenna gain at the grazing angles, thereby restricting the visibility of the low-elevation satellites [37]. It is well known that common choke ring ground planes contribute to undesirable antenna pattern narrowing in the elevation plane which is associated with difficulties of tracking low elevation satellites [38]. Also known is the comparatively narrow frequency bandwidth of the choke grooves structure [39]. This occurs when the grazing angles of an antenna with a flat ground plane coincide with the horizon. Converting the flat ground plane to a convex one, however, improves the antenna radiation pattern near the horizon while keeping the multipath mitigating capability [40]. For full-spectrum GNSS applications, a convex impedance ground plane can be used as an alternative. To enhance the frequency bandwidth of such ground planes, a pin structure is utilized instead of choke grooves [41]. A semi-spherical shape of the ground plane is contributed to provide increased antenna gain for low elevation angles. Instead of common choke grooves, a pin impedance structure is used, resulting in a more consistent frequency response. Convex impedance ground plane provides with less gain pattern roll-off from zenith to horizon and superior rejection of multipath signals [22].

In order to obtain better multipath capability throughout the GNSS band, a convex ground plane with pin structure has been presented in [23]. The antenna design is shown in Figure 12 where it uses an array of vertical convex dipoles capacitively coupled to the antenna feed. The overall antenna performs better in terms of visibility of low-elevation satellites [6].

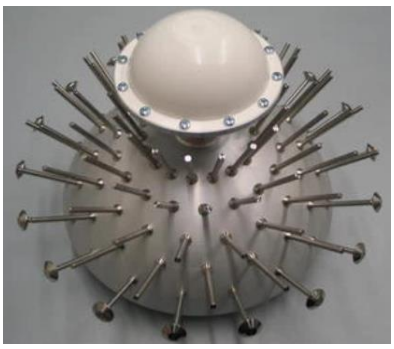

Figure 12. Semi-spherical convex GNSS reference station antenna [23].

2.8 EBG Ground Plane

For many applications, the size and weight of the choke-ring ground plane are drawbacks. There have been developed electromagnetic band gap (EBG) ground planes that are compact, light, and whose thickness is significantly less than a quarter wavelength [42]. The surface of a EBG ground plane is a frequency selective surface and consists of a two-dimensional array of subwavelength metal discs with pins (or subcells) connecting them to the ground plane underneath [43]. Each subcell in the structure can be considered as an LC resonant circuit [44]. The reduction in height is achieved through capacitive loading. High impedance is provided by these EBG surfaces for both polarizations and for all propagation directions [45]. They are sometimes also called artificial magnetic conductors, since the tangential magnetic field is zero at the surface rather than the electric field as in an electrical conductor [46].

In [13], a dedicated low profile antenna for geodesic applications is presented. This type of antenna requires mitigation of multipath signals to achieve sub-centimeter level of precision.

Typically, bulky and heavy choke ring structures have been utilized to mitigate the impacts of multipath interference. The antenna presented consists of a low temperature co-fired ceramic (LTCC) patch antenna immersed in an electromagnetic bandgap (EBG) substrate. The EBG substrate reduces the effects of multipath by blocking the propagation of surface waves [47]. The advantage of printed EBG substrates is that they can be realized in a low-weight, low-cost, and low-profile manner. The photo of low profile antenna using EBG technology is shown as Figure 13.

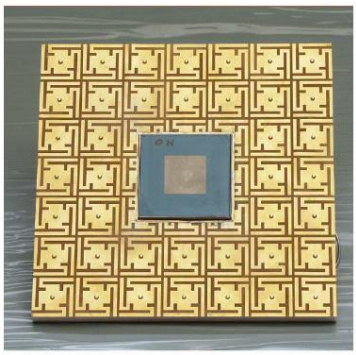

Figure 13. Antenna with cross EBG substrate [13].

It can be concluded that combining EBG technology with antennas can result in low-weight, low-cost, and low-profile alternatives as compared to current commonly used choke ring solutions. Designing antennas employing EBG technology involves certain design rules which have to be taken into account due to the interaction between antenna and EBG-cells. In this, powerful field simulation tools are indispensable.

2.9 Anti-multipath antenna Based on Spiral Antenna and Pinwheel Antenna

The Roke geodetic-grade antenna is a broadband spiral-type antenna designed to support triple-frequency GNSS bands [48]. In order to help minimize multipath, the antenna is a cavity-backed spiral with a unique ground plane structure [49]. Figure 14 depicts the spiral radiating element above the cavity backed structure (i.e.metal can).A cavity backed structure attempts to minimize the reflection off the bottom of the can with special absorbing material within, and what is left reflects in phase with the upward signal in the upper hemisphere. Typically, the radiation spiral elements are situated $\lambda/4$ above the inside bottom of the can structure. (The overall travel distance of the signal inside the can will be 180° and, with a 180 phase shift caused by the normal incident reflection from the metallic can structure, will cause the reflected signal [at zenith] to be in-phase with the upward signal.) [5].

Figure 14. spiral GNSS antenna [48].

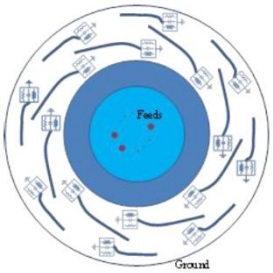

Figure 15. Antenna concept with spiral shaped peripheral parasitic circular array loadings [52].

The NovAtel VEXXIS GNSS-850 antenna is one of the newest GNSS antennas, capable of receiving all GNSS constellation signals in L-band with modest and well-known phase center variations [50][51].A circular patch type element combined with loaded parasitic elements are utilized in this type of planar antenna design, which is illustrated in Figure 15, to maximize bandwidth and reduce gain at low and negative elevation angles [52]. This GNSS antenna provides a reduction of RHCP gain at low elevation angles and significant gain suppression below the horizon to mitigate multipath [53]. Furthermore, the LHCP gain is surprised by typically less than 20 dB from the RHCP. The antenna also exhibits good gain and gain flatness over the GNSS L-band (i.e. <2 dB and 3-5 dBic) as well as consistent gain.

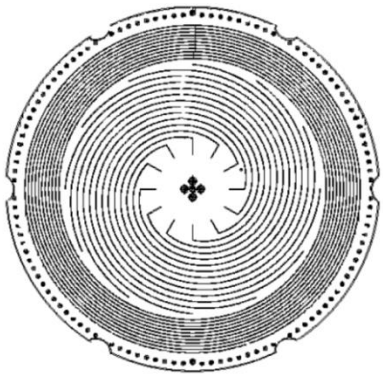

Figure 16. PCB layout for twelve-arm spiral L1 antenna [54].

The pinwheel antenna initially appeared in an ION article published in 2000 [54], and pinwheel antenna is a multi-arm slot antenna, which includes fractal loop configurations at the end of each spiral slot for improving the bandwidth, and NovAtel Corporation has applied for a patent. Multipath, ionospheric delay and antenna phase center variations (PCV) are the most significant sources to error in pseudo-code and carrier phase measurement. Antennas for high-precision measurement applications should ideally be smaller and lighter than traditional "choke ring" antennas. A high performance GPS antenna technology based on "windmill" from NovAtel Corporation has presented, which is characterized by stable phase center and outstanding anti-multipath performance against GPS signals. The antenna is a fixed beam twelve-element antenna composed of aperture coupled spiral groove that can receive GPS right-handed circular polarization signals after optimization. In addition, there are eight concentric groove rings located outside the circumference of the array element, and the spiral groove is to suppress the scattering and reflection from the antenna edge, and achieve good right-circular polarization performance at low elevation angles, as illustrated in Figure 16. This makes it possible to significantly reduce the generation of multipath signals dominated by left-handed circular polarization in low-elevation regions. The antenna has a fairly simple mechanism to establish appropriate phase gradients for all spiral slots to achieve right-handed circular polarization of the entire upper hemisphere. The spiral slot array element has wideband performance and therefore prevents unnecessary phase (group delay) and amplitude modulation of th

e spread spectrum GPS signals found in narrowband antennas. In order to suppress out-of-b and interference, an RF filter is employed in the LNA component of the antenna to limit the fr equency band of the GPS signal. The proposed antenna is fabricated from a single PCB boa rd. Another PCB board is placed under the antenna as a reflector to improve antenna directiv ity and reduce back lobe radiation. The radiation pattern roll down of this antenna is much lar ger than that of traditional GPS patch antenna. Sharp pattern roll down can further reduce th e sensitivity of the antenna to the generated GPS multipath signal. The antenna does not req uire any calibration for a given direction, such as north, due to the natural symmetry of the an tenna structure itself. The antenna configuration consists of an array of coupled spiral slots a rranged in a pinwheel of about 20 cm diameter backed by a microstrip-based multiple-turn sp iral transmission line (Figure 16). The overall antenna structure is compact, lightweight, and has multipath mitigation capability for almost the entire L-band. However, the antenna perfor mance is not uniform across the resonance bandwidth with better performance achieved at h igher frequency. The gain of the antenna at 1.575 GHz (L1) is 6.8 dBiC, but at 1.227 GHz (L 2) it is just 2.8 dBiC.

A wide-band pinwheel antenna designed by NovAtel, Inc. has been presented. In [55], a m iniaturized GPS dual-frequency L1/L2 multi-element adaptive antenna array is designed, in w hich each array unit consists of an aperture coupled spiral slot array. The existing CRPA ant enna adopts the method of microstrip patch layer, which is considerably different from the exi sting CRPA design. The design method of aperture coupled spiral slot array can reduce the mutual coupling between the array elements, thus reducing the overall size of the antenna. Additionally, because of its broadband performance, it will be able to meet the requirements of GPS M-codes. The maximum height of the array antenna is 0.8 ",making it low profile.

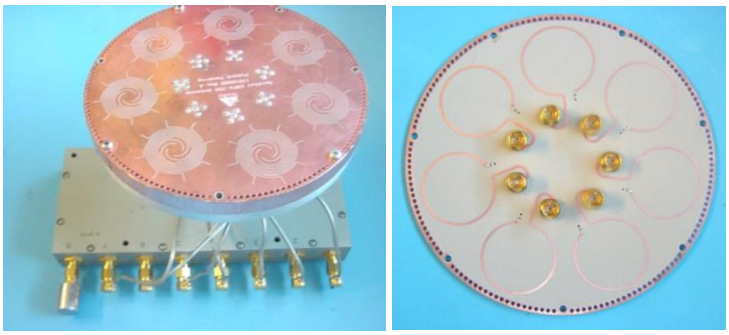

Figure 17. PCB layout for twelve-arm spiral L1 antenna [55].

There have been publications of pinwheel antenna structures [56][57]. In [57], a travelling-wave-fed slot spiral antenna with wide axial-ratio (AR) bandwidth and beamwidth for GNSS applications is proposed in this paper. The evolution procedure of the proposed antenna can be classified into three steps. Firstly, 12 identical spiral slots are arranged concentrically in a compact area, and AR roundness in low elevation plane is improved by virtue of excellent rotational symmetry of slot radiators. Secondly, a two-turn travelling-wave feed line is sequentially coupled to the slots, and wideband response of desired magnitude ratio and phase difference of E_θ and E_ϕ is obtained by optimizing the number and growth rate of microstrip turns. Thirdly, by supporting the antenna with a modified metallic cavity, the CP radiation performance in low elevation plane is significantly improved, and thus a widened AR beamwidth is obtained. Finally, the proposed antenna with satisfactory performance is realized in a diameter of $0.56\lambda_0$ and height of $0.12\lambda_0$, where λ_0 is the free-space wavelength at center frequency 1.4 GHz. Measured bandwidth of |S11| fully covers the entire GNSS bands, and the 3-dB AR bandwidth ranges from 1.14 to 1.67 GHz (37.7%). Additionally, the 3-dB AR

beamwidth exceeds 140 degree at 1.4 GHz. Structure of the proposed antenna is shown as Figure 18. Photos of the antenna prototype are shown as Figure 19.

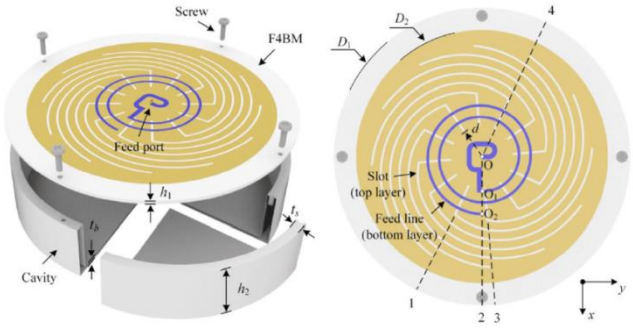

(a) (b)

Figure 18. Structure of the proposed antenna. (a) 3-D exploded view. (b) Top view [57].

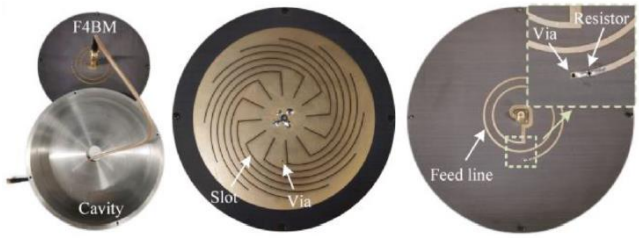

(a) (b) (c)

Figure 19. Photos of the antenna prototype. (a) Exploded view. (b) Top view. (c) Bottom view [57].

2.10 Reduced-Surface-Wave Antenna

The microstrip patch antenna based on the reduced surface wave (RSW) concept can be used as the realization scheme of multipath suppression antenna [58][59][60][61][62].

In [61], it is introduced a GPS microstrip patch antenna designed for dual-band (L1 L2) operation. The antenna design is based on the reduced-surface-wave (RSW) concept and, as a result, is far less susceptible to low elevation angle multipath interference effects than some of the more regularly used high-precision GPS antennas. The simplicity of the design, together with the reduced horizon and backside radiation levels and excellent circular polarization characteristics indicate that this antenna design is a promising candidate for dual-band, high-precision applications [61].

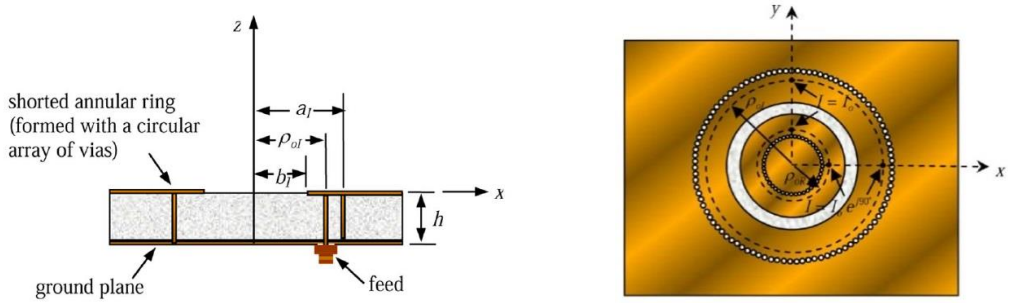

(a) (b)

Figure 20. (a). Side view of a probe-fed inverted shorted-annular-ring reduced-surface-wave patch antenna. (b).The feed configuration used to realize a RHCP RSW antenna [61].

Side view of a probe-fed inverted shorted-annular-ring reduced-surface-wave patch antenna is shown as Figure 20(a). The feed configuration used to realize a RHCP RSW antenna is shown as Figure 20(b).

2.11 Integration in Multifunctional Antenna

Satellite navigation anti-multipath antenna and other types of antennas (such as 4G, 5G, UWB,Bluetooth,SDRS,WiFi,satellite communication) combined into a multifunctional antenna, widely used in various user terminal products. In this way, it is required to have the characteristics of miniaturization, low profile, high integration, and wideband, etc.

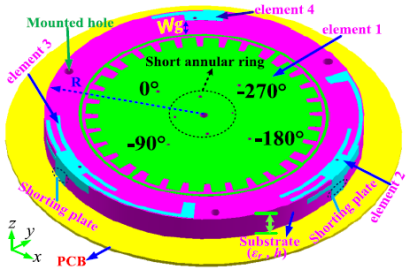

Figure 21. Antenna with cross EBG substrate [63].

In [63], an innovative highly integrated multifunctional global navigation satellite system (GNSS) antenna used for navigation or surveying high-precision area, the fourth-generation (4G) mobile communication, and short-distance wireless communication, is proposed and implemented. The multiple functions are realized with four elements, saying: 1) a low-profile navigation element on one substrate covering all the GNSS bands and 2) two long term evolution multiple-input–multiple-output (LTE-MIMO) elements and one Wi-Fi element uniformly distributed on the edge of the substrate. Utilizing the approaches of short annular ring and capacitance coupling, the bandwidth and AR of the GNSS elements are improved. Additionally, four elements are highly integrated on one substrate. This symmetrical configuration assures the navigation element's low axial ratio (AR) and radiation pattern symmetry, as well as navigation accuracy. Furthermore, to improve the isolation between the GNSS element and other three elements under high integration, these three elements are designed to avoid resonating within the GNSS bands. Because there are no resonance frequencies across the GNSS operation bands for the LTE-MIMO and Wi-Fi elements, the isolation is therefore higher than 20 dB within the entire working band. The TRP of LTE-MIMO elements is better than 17 dBm, while the TIS is approximately −90 dBm. The PCV of the GNSS elements is less than 3.5 mm. The measured peak gains of the GNSS element are 6.0 dBi from 1.16 to 1.28 GHz and 6.5 dBi from 1.52 to 1.62 GHz. The −6 dB impedance bandwidth of the LTE-MIMO elements can cover the frequencies 840–960, 1800–2200, and 2500–2700 MHz. The distance communication of the Wi-Fi element is 80 m. Due to these performances, the proposed antenna has wide range of potential applications in high-precision fields, such as navigation, surveying, and deformation monitoring. Furthermore, the proposed structure can be extended easily to a larger MIMO suited for 5G applications in the sub-6G band.

In [64], it is proposed to develop a wideband GNSS antenna with wide-angle circular polarization and anti-multipath performance. A wide bandwidth is created by using the coupled feeding formed by an arc-T-shaped patch. Eight short-circuit pins are loaded around the radiation patch for widening the 3-dB axial ratio (AR) beamwidth at the GNSS frequencies and reducing size. Furthermore, two sets of bent metal-branches are loaded on the slotted ground for front-back ratio (FBR) enhancement at the GNSS frequencies. To provide uniform circular polarized (CP) excitation with small occupied area, a compact wideband quadrature feed

network with amplitude imbalances within 1 dB and phase imbalances within 5° is designed which covers the GNSS band.

Configuration of the proposed GNSS antenna is shown as Figure 22. Photograph of the fabricated antenna is shown as Figure 23. The results of the measurements indicate that for 10-dB return loss and 3-dB AR, an overlapping bandwidth of more than 45% is obtained. The measured 3-dB AR beamwidths and FBRs are all larger than 200° and 20 dB, respectively, at the frequencies of 1.207 GHz, 1.227 GHz, 1.247 GHz, 1.561 GHz, 1.575 GHz, and 1.602 GHz, illustrating the potential for high precision positioning at GPS L1/L2, BDS B1/B2, GLONASS L1/L2, and Galileo L1/E5b bands.

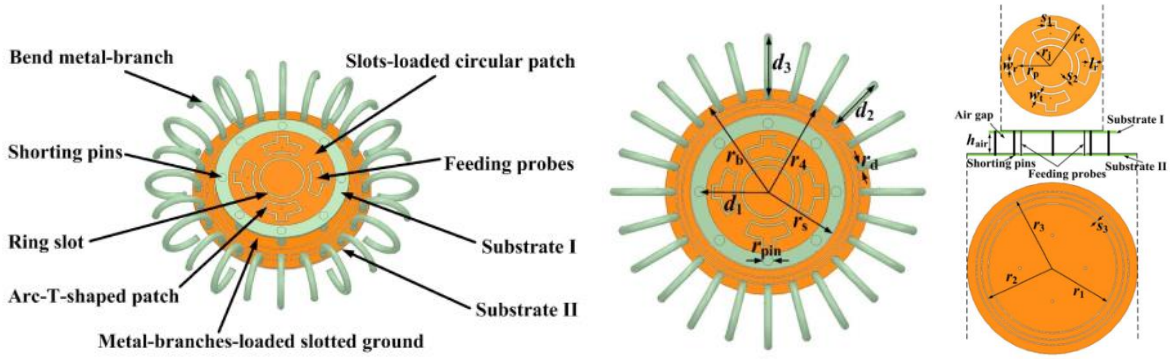

Figure 22. Configuration of the proposed GNSS antenna. (a) 3-D view. (b) Top view. (c) Exploded view (without the bend branches) [64].

Figure 23. Photograph of the fabricated antenna. (a) Top view (b) Bottom view [64].

3. Conclusions and Future Perspectives

This article presents a review of design methodology of a variety of anti-multipath antennas in satellite navigation system. In recent years, researchers have developed a number of novel GNSS anti-multipath antennas. In addition, retracing the origin and evolving trends, large improvements are still possible through efforts in the following aspects: 1) satellite navigation anti-multipath antenna and other types of antennas (such as 4G,5G,UWB,Bluetooth,SDRS,WiFi,satellite communication) combined into a multifunctional antenna, widely used in various user terminal products [65]-[72]. In this way, it is required to have the characteristics of miniaturization, low profile, high integration, and wideband, etc. 2) A variety of types of the existing classical GNSS anti-multipath antenna forms are gradually developing to the direction of miniaturization, light weight, low cost and superior performance.

Authors Contributions: Conceptualization, Qiang Hua; investigation, Jianming Dong; resources, Jianming Dong; data curation, Jianming Dong; writing—original draft preparation, Jianming Dong; writing—review and editing, Jianming Dong and Qiang Hua ; supervision, Qiang Hua.

Funding:

Acknowledgements:

Conflicts of Interest: Declare any potential conflicts of interest or state “The authors declare no conflict of interest”.

Appendix A

References

1. B. Rama Rao, W. Kunysz, R. Fante, K. McDonald, 2013. *GPS/GNSS Antennas* (pp.1-91), Artech House.
2. E.D.Kaplan, and Hegarty C.J., 2006, *Understanding GPS* (pp.1-91), Second Edition, ARTECH HOUSE Inc, Norwood, MA.
3. Chris.Rizos,2010;GPS,GNSS and the Future, *Manual of Geospatial Science and Technology* (pp.259-281),Editor:J.D.Bossier;Second Edition;CRC Press;Boca Raton.
4. Bernhard Hofmann-Wellenhof, Herbert Lichtenegger, Elmar Wasle, 2008, GNSS—Global Navigation Satellite Systems; *GPS, GLONASS, Galileo and More* (pp.309-430), Springer Verlag Wien.
5. Mohinder S.Grewal,Angus P.Andrews, Chris G.Bartone, *Global Navigation Satellite Systems, Inertial Navigation, and Integration* (pp.266), Wiley. Boston | London.
6. Peter J.G.Teunissen,Oliver Montenbruck,2017.*Handbook of Global Navigation Satellite Systems* (pp.515). Springer. Boston | London.
7. Hein, G, W., J. A. Avila-Rodriguez, S. Wallner, B. Eisfeller, P. Thomas, P. Hard; 2007. Envisioning a Future GNSS System of Systems, *Inside GNSS*, Part 1, pp. 58-67.
8. J.M.Tranquilla, J.P.Carr, and H.M.Al-Rizzo,1994. Analysis of a choke ring ground plane for multipath control in global positioning system (GPS) applications, *IEEE Transactions on Antenna and Propagation*, vol. 42, no. 7, pp.905–911.
9. W. E. McKinzie, R. B. Hurtado, B. K. Klimczak and J. D. Dutton, 2002.Mitigation of multipath through the use of an artificial magnetic conductor for precision GPS surveying antennas, *IEEE Antennas and Propagation Society International Symposium* (*IEEE Cat. No.02CH37313*), San Antonio, TX, USA, pp. 640-643 vol.4.
10. C.C.Tchapwou and T.Bertuch, 2007. Investigation of EBG surface performance for high-precision GPS applications, *Electronic Letters*, vol.43, no.24, pp.1327–1329.
11. Mohamed K. Emara, Julien Hautcoeur, Gyles Panther, Jim S. Wight, and Shulabh Gupta,2019, Surface Impedance Engineered Low-Profile Dual-Band Grooved-Dielectric Choke Ring for GNSS Applications. *IEEE Transactions on Antenna and Propagation*, vol.67, no.3, pp. 2008-2011.
12. Y. Lee, S. Ganguly, and R. Mittra, Multi-band L5-capable GPS antenna with reduced backlobes, 2005, in Proc. *IEEE Antennas and Propagation Society Symp.*, Washington, DC,Jul.3-8,2005,vol.1A,pp.438-441.
13. Rens Baggen, Marta Martínez-Vázquez, Jens Leiss, Sybille Holzwarth, Luca Salghetti Drioli, and Peter de Maagt, 2008. Low Profile GALILEO Antenna Using EBG Technology. *IEEE Transcations on Antenna and Propagation,* vol.56, no.3, pp. 667-674.
14. UNAVCO(2012),Choke+ring+antenna+calibrations.https://facility.unavco.org/kb/questions/311/Choke+Ring+Antenna+Calibrations (visited 28 May 2012).
15. M. Maqsood, S. Gao, T. Brown, and M. Unwin, 2010. Effects of ground plane on the performance of multipath mitigating antennas for GNSS, in *2010 Loughborough Antennas & Propagation Conference*, Loughborough, UK, pp. 241–244.

16. Filippov.V., Tatarnicov, D., Ashjaee,J. et al.(1998). The first dual-depth dual-frequency choke ring. In: *Proceedings of the 11th International Technical Meeting of the Satellite Division of The Institute of Navigation* (*ION GPS 1998*), 1035-1040.TN: Nashville.
17. F.Khosravi, H.Moghadas, and P.Mousavi, 2015. A GNSS Antenna With a Polarization Selective Surface for the Mitigation of Low-Angle Multipath Interference, *IEEE Transcations on Antenna and Propagation*, vol. 63,no. 12, pp. 5287–5295.
18. Javad,2012. Choke ring theory.
19. Thornberg, D.B., Thornberg, D.S.,DiBenedetto, M.F.et al.,2003.LAAS integrated multipath-limiting antenna. *ION Navigation Journal* 50 (2):117-130.
20. Kunysz, W. ,2003. A three dimensional choke ring ground plane antenna. In: *ION GPS/GNSS 2003*, Portland, OR (9-12 September 2003), 1883-1888.
21. Ehsan Taghdisi, Mohammad Saeid Ghaffarian, Rashid Mirzavand, 2022 March. Low-Profile Substrate Integrated Choke Rings for GNSS Multipath Mitigation, in *IEEE Transcations on Antenna and Propagation*, vol.70, no.3, pp. 1706-1718.
22. M. Maqsood, S. Gao, T. W. C. Brown, M. Unwin, R. de vos Van Steenwijk and J. D. Xu, 2013 May. A Compact Multipath Mitigating Ground Plane for Multiband GNSS Antennas, in *IEEE Transactions on Antennas and Propagation*, vol. 61, no. 5, pp. 2775-2782.
23. L. Boccia, G. Amendola, G. Di Massa, and L. Giulicchi, 2001, Shorted annular patch antennas for multipath rejection in GPS-based attitude determination systems, *Microw. Opt. Tech. Lett.*, vol. 28, no. 1, Jan.
24. M.Maqsood, S.Gao, T.Brown, J.Xu, and J.Li, 2012 Mar. Novel multipath mitigating ground planes for multiband global navigation satellite system antennas, in *Proc. 6th Eur. Conf. antennas Propag. (EUCAP)*, pp. 1920–1924.
25. B. W. Parkinson, J. J. Spilker, Jr., P. Axelrad, and P. Enge, 1996. Global positioning system: Theory and applications, *Amer. Institute Astronautics Aeronautics*, vol.1, pp. 547–566, 3rd ed., ch.14.
26. C. C. III Counselman,1999 Jan. Multipath-rejecting GPS antennas, *IEEE Proc. Special Issue GPS Global Positioning Syst.*, vol. 87, no.1, pp. 86–91.
27. A. M. Dinius,1995.*GPS Antenna Multipath Rejection Performance* Massachusetts Institute of Technol., Lincoln Lab., Cambridge, MA, Rep.ATC-238, Aug., vol. 70.
28. B. R. Rao, J. H. Williams, E. N. Rosario, and R. J. Davis, GPS microstrip antenna array on a resistivity tapered ground plane for multipath mitigation, [Online]. Available: http://www.mitre corporation.com/work/tech_papers.
29. T. Milligan and P. K. Kelly, 1996, Optimization of ground plane for improved GPS antenna performance, *IEEE Antennas and Propagation Society International Symposium*. 1996 Digest, Baltimore, MD, USA, pp. 1250-1253 vol.2.
30. F.Scire-Scappuzzo and S.N.Makarov, 2009. A Low-multipath wideband GPS antenna with cutoff or non-cutoff corrugated ground plane, *IEEE Transcations on Antenna and Propagation,* vol.57, no.1, pp.33-46.
31. H. R. Khaleel, H. Al-Rizzo, A. Isaac and A. Bihnam, 2014,Multipath mitigation in high precision GPS systems using Artificial Magnetic Conductors, *2014 IEEE Antennas and Propagation Society International Symposium* (*APSURSI*), Memphis, TN, USA, pp. 432-433.
32. TrimbleNavigationLimited,[Online].Available:http://www.trimble.com/l1l2chokering.shtml.
33. C. C. Counselman,1999,Multipath-rejecting GPS antennas, in *Proceedings of the IEEE*, vol. 87, no. 1, pp. 86-91, Jan. 1999.
34. Westfall,B.,1997.Antenna with R Card Ground Plane, U.S.Patent #5,694,136,USPTO.

35. Lennen,G.,W.Hand, and B.Westfall,1996.GPS Recevier with N-point Symmetrical Feed Double Frequency Patch Antenna, U.S.Patent #5,515,957,USPTO.
36. B. R. Rao, M. N. Solomon, M. D. Rhines, L. J. Teig, R. J. Davis and E. N. Rosario, Research on GPS antennas at Mitre, 1998, *IEEE 1998 Position Location and Navigation Symposium* (Cat. No.98CH36153), Palm Springs, CA, USA, pp. 634-641.
37. Tatarnikov DV,Filippov VS,Soutiaguine IV,Astakhov AV,Stepanenko AP,Shamatulsky PP,2005.Multipath mitigation by conventional antennas with ground planes and passive vertical structures. *GPS Solutions* 9(3):194–201.
38. Tatarnikov DV,2008. Ground planes for high precision GNSS antennas. Part 1. Conductive and impedance ground planes. Antennas 4(131):6–19 Moscow, Radiotechnika (in Russian).
39. D.Tatarnikov, A.Stepanenko, A.Astakhov, V.Filippov, 2010. Compact circular polarized antenna with expanded frequency bandwidth, Patent RF No.2380799.
40. D.Tatarnikov, A. Astakhov, A. Stepanenko, 2011. Broadband convex impedance ground planes for multisystem GNSS reference station antennas, *GPS Solutions 15(2)*, 101–108.
41. D. Tatarnikov, A. Astakhov and A. Stepanenko, 2011, Convex GNSS Reference station antenna, *2011 International Conference on Multimedia Technology*, Hangzhou, China, pp. 6288-6291.
42. Sievenpiper. D, 2006. Review of the Theory, Fabrication, and Application of High Impedance Ground Planes, in *Metamaterials: Physics and Engineering Explorations*, N.Engheta and R.K.Ziolkowski(eds.),Hoboken,NJ:John Wiley&Sons,pp.287-309.
43. G. Goussetis, A. P. Feresidis and J. C. Vardaxoglou, 2006.Tailoring the AMC and EBG characteristics of periodic metallic arrays printed on grounded dielectric substrate, in *IEEE Transactions on Antennas and Propagation*, vol. 54, no. 1, pp. 82-89.
44. J.-M. Baracco, L. Salghetti-Drioli and P. de Maagt, 2008. AMC Low Profile Wideband Reference Antenna for GPS and GALILEO Systems, in *IEEE Transactions on Antennas and Propagation*, vol. 56, no. 8, pp. 2540-2547.
45. N. Padros, J. I. Ortigosa, J. Baker, M. F. Iskander and B. Thornberg, 1997. Comparative study of high-performance GPS receiving antenna designs, in *IEEE Transactions on Antennas and Propagation*, vol. 45, no. 4, pp. 698-706.
46. Zhang,Y.,M. Younis, and C. Fischer, et al.,2003.Planar Artificial Magnetic Conductors and Patch Antennas, *IEEE Transcations on Antenna and Propagation*, Vol. 51, No. 10, October pp. 2704–2712.
47. A. P. Feresidis, G. Goussetis and J. C. Vardaxoglou, 2004. Metallodielectric arrays without vias as artificial magnetic conductors and electromagnetic band gap surfaces, IEEE Antennas and Propagation Society Symposium, Monterey, CA, USA, pp. 1159-1162 vol.2.
48. Roke,2012. Roke triple GNSS geodetic-grade antenna.
49. Krantz, E., Riley, S., and Large,P.,2001.The design and performance of the zephyr geodetic antenna, in *Proceedings of the 14th International Technical Meeting of the Satellite Division of The Institute of Navigation* (*ION GPS 2001*), Salt Lake City, UT(11-14 September 2001),1942-1951.
50. Granger,R. and Simpson,S.,2008. An analysis of multipath mitigation techniques suitable for geodetic antennas, in *Proceedings of the 21st International Technical Meeting of the Satellite Divison of The Institute of Navigation* (*ION GNSS 2008*), Savannah, GA (16-19 September 2008),2755-2765.
51. Vexxis gnss-500 series antennas. https://www.novatel.com/products/gnss-antennas/vexxis-series-antennas/vexxis-gnss-500-series-antennas/,2016.

52. Yang, N. and Freestone, J. (2016). High-performance GNSS antennas with phase-reversal quadrature feeding network and parasitic circular array. In: *Proceedings of the 29th International Technical Meeting of the Satellites Division of The Institute of Navigation* (*ION GNSS+2016*), Portland, Oregon (September 2016), 364-372.
53. Gerein,N. and Freestone,J.(2019). NovAtel GNSS-800 Antenna Information files.
54. Waldemar Kunysz, NovAtel Inc., 2000. High Performance GPS Pinwheel Antenna. *ION*, *210*, pp.135-144.
55. Waldemar Kunysz, NovAtel Inc., 2001. Advanced Pinwheel Compact Controlled Reception Pattern Antenna (AP-CRPA) designed for Interference and Multipath Mitigation. *ION GNSS+ 2001*.
56. Novatel, GPS-704X Antenna Design and Performance [Online]. Available: http: // webone. novatel.ca/assets /Documents/Papers/GPS-704x White Paper.pdf
57. Zeng-Pei Zhong, Xiao Zhang, 2021. A Travelling-Wave-Fed Slot Spiral Antenna With Wide Axial-Ratio Bandwidth and Beamwidth for GNSS Applications, *IEEE Open Journal of Antenna and Propagation,* vol. 2, pp. 578-584.
58. Lorena I. Basilio, Richard L. Chen, Jeffery T. Williams, David R. Jackson, 2018. A New Planar Dual-Band Tunable AMC Structure for GNSS Antennas and Its Performance Trade-Offs. *18th International Symposium on Antenna Technology and Applied Electromagnetics* (*ANTEM*).
59. Mohamed K. Emara, Shulabh Gupta, Julien Hautcoeur, Gyles Panther, Jim S. Wight, 2007. A Low-Profile Dual-Band GPS Antenna Designed for Reduced Susceptibility to Low-Angle Multipath, *IEEE Transactions on Antenna and Propagation*, vol.55, no.8.
60. L. I. Basilio, J. T. Williams, D. R. Jackson, and M. A. Khayat, 2005. A comparative study of a new GPS reduced-surface-wave antenna, *IEEE Antennas and Wireless Propagation Letters*, vol. 4, pp. 233–236.
61. L.I. Basilio, 2003. New GPS Antennas Designed for Reduced Multipath Susceptibility, Ph.D. Dissertation, University of Houston, Houston, TX.
62. H. Liu, S. Fang, and Z. Wang, 2013. A novel multimode reduced-surface-wave antenna for GNSS applications, *IEEE Antennas and Wireless Propagation Letters*, vol.12, pp.1618–1621.
63. Jia Wei, Shaowei Liao, Quan Xue, 2022. High Integrated Multifunctional Antenna for Global Navigation Satellite System. *IEEE Transcations on Antenna and Propagation,* vol.70, No.12.
64. H. Liu, J. Wang, Z. Zhao, Z. Wang and S. Fang, 2023.Design of Wideband GNSS Antenna With Wide-Angle Circular Polarization and Anti-Multipath Performance for High Precision Marine Positioning, in *IEEE Transactions on Vehicular Technology*, vol. 72, no. 5, pp. 6281-6293.
65. Y. Liu, Z. Ai, G. Liu and Y. Jia, 2019. An Integrated Shark-Fin Antenna for MIMO-LTE, FM, and GPS Applications, in *IEEE Antennas and Wireless Propagation Letters*, vol. 18, no. 8, pp. 1666-1670.
66. O. -Y. Kwon, R. Song and B. -S. Kim, 2018. A Fully Integrated Shark-Fin Antenna for MIMO-LTE, GPS, WLAN, and WAVE Applications, in *IEEE Antennas and Wireless Propagation Letters*, vol. 17, no. 4, pp. 600-603.
67. Q. Wu, Y. Zhou and S. Guo, 2018. An L-Sleeve L-Monopole Antenna Fitting a Shark-Fin Module for Vehicular LTE, WLAN, and Car-to-Car Communications, in *IEEE Transactions on Vehicular Technology*, vol. 67, no. 8, pp. 7170-7180.
68. I. Goncharova and S. Lindenmeier, 2015. A high efficient automotive roof-antenna concept for LTE, DAB-L, GNSS and SDARS with low mutual coupling, 9th European Conference on Antennas and Propagation (EuCAP), Lisbon, Portugal, 2015, pp. 1-5.

69. E. Ghafari et al., 2014. A vehicular roof top, shark-fin, multiband antenna for the GPS/LTE/cellular/DSRC systems, in Proc. *IEEE-APS Top. Conf. Antennas Propag. Wireless Commun.* (*APWC*), pp. 237–240.
70. D. Huang, Z. Du, and Y. Wang, 2019. A quad-antenna system for 4G/5G/GPS metal frame mobile phones, *IEEE Antennas and Wireless Propagation Letters*, vol. 18, no. 8, pp. 1586–1590.
71. A. Abdalrazik, A. Gomaa, and A. Ahmed Kishk, 2021. A hexaband quadcircular-polarization slotted patch antenna for 5G, GPS, WLAN, LTE, and radio navigation applications, *IEEE Antennas and Wireless Propagation Letters*, vol. 20, no. 8, pp. 1438–1442.
72. H. S. Singh and M. Agarwal, 2014. A quad-band compact diversity antenna for GPS L1/Wi-Fi/LTE2500/WiMAX /HIPERLAN1 applications, *IEEE Antennas and Wireless Propagation Letters*, vol. 13, pp. 249–252.